Power Consumption Estimation of Digital Predistortion based on Spiking Neural Networks

Siqi Wang, Pietro M. Ferreira, Julien Sarrazin, A. Benlarbi-Delai

Power Consumption Estimation of Digital Predistortion based on Spiking Neural Networks

Siqi Wang, Pietro Maris Ferreira, Julien Sarrazin, Aziz Benlarbi-Delai

Sorbonne Université, CNRS, Lab. de Génie Electrique et Electronique de Paris, 75252, Paris, France
Université Paris-Saclay,CentraleSupélec,CNRS,Lab. de Génie Electrique et Electronique de Paris,91192,Gif-sur-Yvette,France

***Abstract*—Different neuromorphic circuits have been proposed in recent years for low-power implementation of spiking neurons. However, there are very few clear quantitative studies on the power consumed by these spiking neurons as well as their networks. In this paper, we present a study on power consumed by some recently designed analog electronic neurons. An application of different structures of spiking neural network (SNN) to digital predistortion for MIMO antenna array linearization through over-the-air (OTA) feedback is taken as an example for numerical analysis, which demonstrates the effectiveness of SNN.**

***Index Terms*—Artificial intelligentce (AI), digital predistortion, energy efficiency, MIMO, neuromorphic, OTA, spiking neural networks (SNN)**

I. Introduction

Inspired by the biological behavior of the brain cortex, the spiking neural networks (SNN) transmit and process information in the form of spike trains. In a cortex neuron, the passing of Sodium (Na^+) and Potassium (K^+) ions through the membrane generates a biological current I_{ex} [1] which increases or decreases the membrane voltage V_m. When V_m exceeds a given threshold V_T, the neuron fires a spike which is then sent to other connected neurons through the synapses. After firing the spike, V_m falls down quickly back to a rest value V_c. This electric behavior in the neuron has been described by partial differential equations as the Hodgkin-Huxley (HH) model [2] and Morris-Lecar (ML) model [3]. The LIF model is a simplified version which has low computational burden [4]. Since the membrane can be represented by capacitors, an equivalent electronic neuron can be designed according to these partial differential equations [5]. Recently some studies on neuromorphic circuits provide solutions to highly energy efficient spiking neurons [6]–[8].

Thanks to the sparsity of signals and simple computation, the SNN is considered advantageous in power consumption compared with classical neural networks. In [9], the SNN is reported having over 100 times higher energy efficiency than the ANN when implemented on the same hardware. Different applications of SNN have been proposed. Most of them concentrated on classical problems such as image recognition [10] and video processing [11]. In [12], the SNN is used for one-dimension data regression in the linearization of a radiofrequency (RF) power amplifier (PA) as a digital predistortion (DPD).

The PA consumes the majority of power in modern wireless communication systems [13]. Enhancing the PA's energy efficiency is crucial especially for 5G and beyond networks. However, this demands the PA to work close to its saturation, which brings strong distortion to the transmitted signal [14]. The DPD is one of the most commonly used technique to address the PA linearization problem [15]. In massive multi-input multi-output (MIMO) systems for 5G, it is fastidious and impractical to linearize of the system with beamforming through knowing the behavior models for each of the PAs in the antenna array as in classical single PA scenario. Observation feedback through over-the-air (OTA) method can help to linearize the PA array and the propagation channel together [16]. The power consumption is a key factor to consider in designing the DPD [17]. In the literature, some simplified versions based on Volterra series have been proposed in past decades, such as memory polynomial (MP) [18], generalized memory polynomial (GMP) [19], dynamic-deviation-reduction (DDR) model [20], and decomposed vector rotation (DVR) model [21]. Block-oriented non linear (BONL) systems [22] and neural networks [23] have also been studied. The power consumption of these DPD techniques is usually estimated through counting the running complexity in terms of number of floating point operations per sample (Flops) [24]. With the development of neuromorphic circuits, the computational operation in an SNN may consumes much less than a Flops. Estimating the electronic neuron's power consumption in early design can makes it comparable without Flops.

In this paper, we first linearize a 10-PA array followed by a line-of-sight (LOS) channel with an SNN in simulation. Then we estimate the power consumption of this SNN based on electronic neurons (e-neurons) designed in [25] and [26]. A polynomial fitting is used to interpolate the measured dataset from Post-layout simulation.

This paper is organized as follows. In Section II, the LIF neuron is presented and its power consumption is estimated. The test models of PAs and LOS channel are presented in Section III. In Section IV, we introduce a 2-layer SNN-DPD and derive a mathematical expression to estimate its power consumption. Finally, the conclusion is given in Section V.

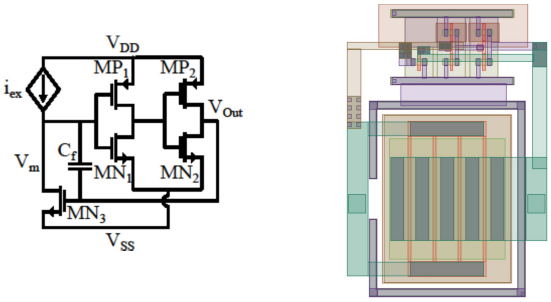

(a) (b)

Fig. 1: Electronic circuit and layout of a LIF neuron in [25]: (a) Electronic circuit of a LIF neuron; (b) Layout of a LIF neuron (6.56 × 4.33 μm^2).

II. Spiking Neurons

A. Spiking neuron models

The variation of membrane voltage V_m as a function of excitation current I_{ex} can be described by LIF model:

$$\begin{cases} \frac{dV_m}{dt} & = \frac{I_{\text{ex}}}{C} + \frac{V_0 - V_m}{RC} \\ V_m & = V_c, \text{ if } V_m > V_s \end{cases} \tag{1}$$

where V_s is the threshold voltage to fire a spike, V_c is the rest voltage after firing a spike, R and C are equivalent resistor and capacitor of the membrane, V_0 is a biased voltage on the membrane.

The ML model is given in [3] as follows

$$\begin{cases} I_{\text{ex}} & = C\frac{dV_m}{dt} + g_L(V_L) + g_{\text{Ca}}M(V_m - V_{\text{Ca}}) \\ & \quad + g_{\text{K}}N(V_m - V_{\text{k}}) \\ \frac{dM}{dt} & = \lambda_M(V)[M_\infty(V - M)] \\ \frac{dN}{dt} & = \lambda_N(V)[N_\infty(V - N)] \end{cases} \tag{2}$$

where C is the membrane capacitance, g_{Ca} and g_{K} are maximum conductance of channels for Ca and K ions respectively, G_L is the leakage conductance, V_{Ca} and V_{K} are Nernst potentials for Ca and K ions respectively, V_L is the leakage potential, M and N are activation coefficients, the variables (λ_M, λ_N) are functions of V_m.

B. Power consumption of electronic spiking neurons

According to the models of spiking neuron, different circuits for electronic neurons (e-neurons) have been designed. A LIF circuit design from [25] is depicted in Fig. 1. The energy consumed during the period of one spike T is equal to integration of the drain-to-source current I_{DS} times the supply voltage V_{DD}:

$$E = \sum_i^{N_{\text{inv}}} V_{\text{DD}} \int_0^T I_{\text{DS},i}(t)dt. \tag{3}$$

where N_{inv} is the number of CMOS inverters. By solving (1), we can obtain the expression of membrane voltage in a LIF neuron as follows:

$$V_m(t) = (V_0 + I_{\text{ex}}R)(1 - e^{-\frac{t}{RC}}) + V_c \tag{4}$$

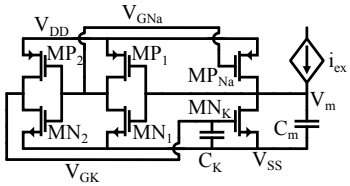

(a) Electronic circuit of an ML neuron.

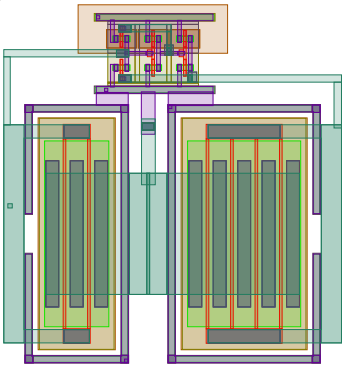

(b) Layout of an ML neuron (8.21 × 7.52 μm^2).

Fig. 2: Electronic circuit and layout of an ML neuron in [26].

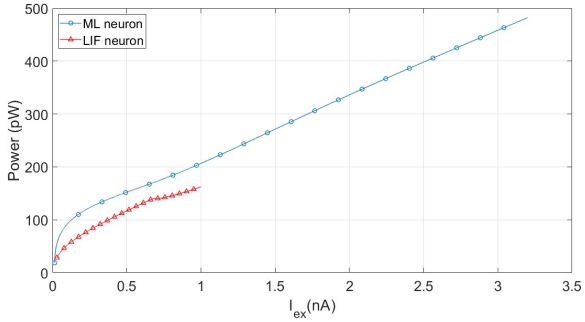

Fig. 3: Power of an e-neuron as a function of excitation current I_{ex} estimated in Post-layout simulation.

where t is the time and we regard $V_0 = V_c$ at time $t = 0$. Knowing $I_{\text{DS},i}$=$(V_{\text{DD}} - V_m(t))g_i$ where g_i is the conductance of PMOS in the i-th inverter, and

$$\begin{aligned} &\int_0^T V_m(t)dt = (V_0 + I_{\text{ex}}R)T - RCV_s \\ &= (V_0 + I_{\text{ex}}R)RC\ln(\frac{V_0 + I_{\text{ex}}R}{V_0 + I_{\text{ex}}R - V_s}) - RCV_s, \end{aligned} \tag{5}$$

we compute the power by (3)/T as follows:

$$P = \sum_i^{N_{\text{inv}}} g_i V_{\text{DD}}^2 - g_i V_{\text{DD}}\big((V_0 + I_{\text{ex}}R) - \frac{RCV_s}{T}\big). \tag{6}$$

To be noticed, the value of I_{ex} is usually smaller than I_{DS}.

An ML circuit in [26] and its layout design are depicted in Fig. 2. With these layout of e-neurons, one can estimate the power consumption of spiking neurons in Post-layout simulation. The power consumption of LIF and ML circuits as a function of the input excitation current I_{ex} is depicted in Fig. 3 where V_{DD}=200mV. The blue curve representing the power consumption of an ML neuron is smooth. The red curve representing the power consumption of a LIF neuron

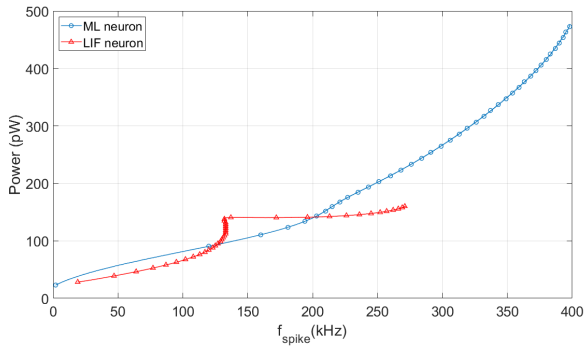

Fig. 4: Power of an e-neuron as a function of output spiking rate f_{spike} estimated in post-layout simulation(PLS) from Virtuoso Cadence.

has a breakpoint when I_{ex}=0.68 nA. To avoid the complex expression of R in transistors, we can use the following polynomial approximations to estimate the power consumption in pW of LIF and ML neurons respectively:

$$P_{\text{LIF}}^{(\text{in})}(I_{\text{ex}}) = \begin{cases} \sum_{k=0}^{5} a_{1,k} I_{\text{ex}}^{k}, & \text{if } I_{\text{ex}} \in [0 \text{ nA}, 0.68 \text{ nA}] \\ \sum_{k=0}^{3} a_{2,k} I_{\text{ex}}^{k}, & \text{if } I_{\text{ex}} \in (0.68 \text{ nA}, 1 \text{ nA}] \end{cases} \tag{7}$$

where a_1=[17.50, 458.9, -1484, 3580, -4309, 2016], a_2=[500.7, -1335, 1583, -586.4], with MSE of 0.22 pW, and

$$P_{\text{ML}}^{(\text{in})}(I_{\text{ex}}) = \sum_{k=0}^{10} b_k I_{\text{ex}}^{k}, \tag{8}$$

where b=[34.18, 800.5, -3049, 7254, -10481, 9688, -5825, 2261, -545.9, 74.45, -4.379], I_{ex} ∈[0, 3.2nA], with MSE of 0.99 pW. We can then estimate the power consumption of the input layer of an SNN if we know the input of every neuron:

$$P = \sum_{h=1}^{N_{\text{in}}} P^{(\text{in})}(I_{\text{ex},h}), \tag{9}$$

where N_{in} is the number of neurons in the input layer.

In Fig. 4, the power consumption of LIF and ML circuits as a function of the output spiking rate f_{spike} is presented. The power consumption in pW of a LIF neuron has a breakpoint when f_{spike}=133 kHz. If we know the output of every neuron, we can then estimate the power consumption of the output layer of an SNN as

$$P = \sum_{j=1}^{N_{\text{out}}} P^{(\text{out})}(f_j), \tag{10}$$

where N_{out} is the number of neurons in the output layer, and the polynomial approximations for LIF and ML neurons are respectively:

$$P_{\text{LIF}}^{(\text{out})}(f) = \begin{cases} \sum_{k=0}^{4} a_{1,k} f^{k}, & \text{if } f \in [0 \text{ kHz}, 133 \text{ kHz}] \\ \sum_{k=0}^{3} a_{2,k} f^{k}, & \text{if } f \in (133 \text{ kHz}, 271 \text{ kHz}] \end{cases} \tag{11}$$

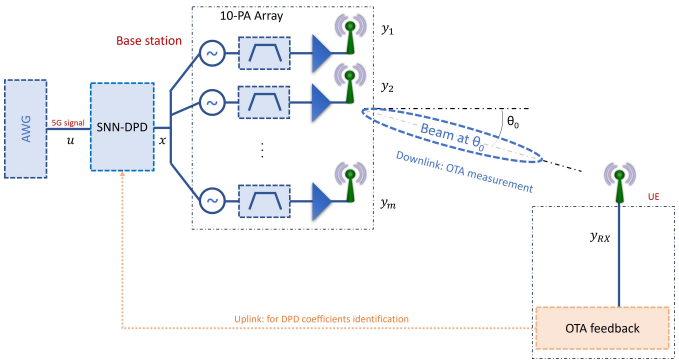

Fig. 5: Antenna array system linearized by DPD with OTA feedback.

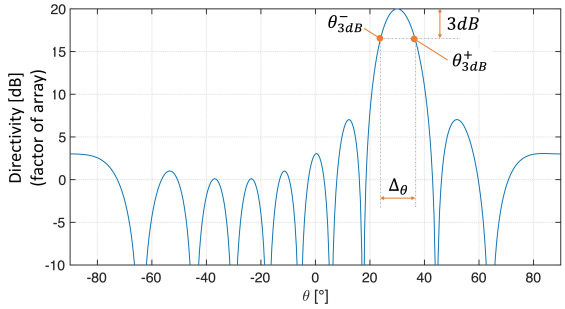

Fig. 6: Antenna Array Radiation Diagram.

where a_1=[121.3, -6.946, 0.1769, -0.0017, $5.917e^{-6}$], a_2=[21.27, 2.024, -0.0114, $2.147e^{-5}$], with MSE of 5.2 pW, and

$$P_{\text{ML}}^{(\text{out})}(f) = \sum_{k=0}^{10} b_k f^{k}, \tag{12}$$

where b=[34.18, 800.5, -3049, 7254, -10481, 9688, -5825, 2261, -545.9, 74.45, -4.379], f ∈[0, 400 kHz], with MSE of 0.99 pW.

According to (9)-(10), the power consumption of the 2-layer SNN using neuromorphic circuits can be expressed as

$$P = \sum_{h=1}^{N_{\text{in}}} P^{(\text{in})}(I_{\text{ex},h}) + \sum_{j=1}^{N_{\text{out}}} P^{(\text{out})}(f_j). \tag{13}$$

III. PA AND CHANNEL MODELS

The antenna array system is shown in Fig. 5. The signal u is the signal to be transmitted generated by the baseband unit. The signal x is the predistorted signal calculated by the DPD and is sent to the antenna array with N phase shifters followed by N PA and N antennas allowing beam steering in the direction θ_0. The signal y is the signal received by a user (UE) equipped with a single antenna. It is sent back to the base station via the OTA return channel to calculate the DPD coefficients. The PA model used is a Wiener structure: a filter followed by a Saleh model. A random variation is added to the phase of the coefficients of the Saleh model of each PA so that the characteristics of the PAs are different. The propagation channel between each antenna in the network and the UE follows a line-of-sight (LOS) model.

The transfer function of each PA can be represented by a Hammerstein structure as below:

$$w(n) = f\big(u(n)\big) \tag{14}$$

$$x(n) = \sum_{l=0}^{L} b_l w(n-l), \tag{15}$$

where $w(n)$ is an intermediate signal between 2 stages of the model, $f(.)$ represents a nonlinear function which is produced by the Saleh model [27]:

$$\begin{aligned} A(w(n)) &= \frac{\alpha_A |u(n)|}{1+\beta_A |u(n)|^2} \\ \phi(w(n)) &= \frac{\alpha_\phi |u(n)|^2}{1+\beta_\phi |u(n)|^2}, \end{aligned} \tag{16}$$

where α_A, β_A, α_ϕ and β_ϕ are constants, $A(.)$ and $\phi(.)$ represent the amplitude and the phase respectively.

The LOS channel model h_m is applied as follows:

$$y_{RX}(n) = \sum_{m=0}^{9} h_m y_m(n), \tag{17}$$

where y_m is the output of the m-th antenna, y_{RX} is the signal received by the UE. A phase weighting vector is introduced to generate a beam towards $\theta_0 = 30°$, as shown in Fig. 6.

IV. Application of SNN on MIMO OTA Linearization

In [12], authors have proposed to implement 2-layer SNN-DPD technique in frequency domain. In this paper, we include the channel information in the SNN-DPD which is identified with feedback data through OTA. Since the LOS channel brings only additional memory effects to the PA models, the frequency domain model needs only adjustments on phase rotations of subcarriers as indicated in [28]. The SNN-DPD is trained through spike-timing-dependent plasticity (STDP) with the remote supervised method (ReSuMe) proposed in [29]. We use an augmented iterative learning control algorithm (AILC) [30] to obtain a target data for the supervisor layer, which results in a linearized signal at the receiver through OTA.

The network contains 10 antennas associated with 10 PAs. The input signal u is a 20MHz band LTE waveform. The linearization performance by the SNN is illustrated by the spectrum received in a LOS channel in Fig. 7. In the direction $\theta_0 = 30°$, the spectrum is given with and without DPD.

The performance of SNN-DPD is given in Table I. The linearization accuracy is evaluated with adjacent channel leakage ratio (ACLR). Since the SNN in this paper uses ML model as neurons, the power consumption is estimated using (8) and (12). We have tested the SNN with different neurons in the input and output layers. Since the length of dataset is 20 000 samples and the sampling rate is 200 MHz, according to fast Fourier transform (FFT) the number of frequency samples of 20 MHz LTE is 2000. After splitting the real and imaginary part for the SNN input data preparation, there are 4000 samples to be fed to the SNN input layer. The frequency

TABLE I: Performance comparison of DPD models

	No DPD	SNN 1	SNN 2	SNN 4	AILC
ACLR.L (dBc)	-27.7	-45.4	-42.2	-42.5	-58.6
ACLR.U (dBc)	-28.1	-45.4	-43.8	-41.7	-58.2
[N_{in},N_{out}]	-	[$4e^3$,$12e^3$]	[$2e^3$,$6e^3$]	[$1e^3$,$3e^3$]	-
Power (μW)	-	4.1	2.0	1.0	-

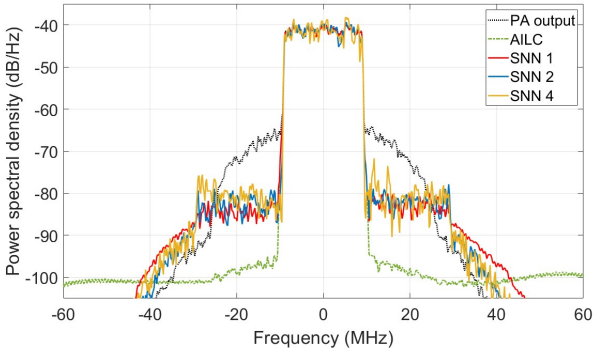

Fig. 7: Baseband spectrum received by UE with LOS channel.

samples of predistorted signal covers at least 3 times of the bandwidth of the input signal. Thus there are 12 000 samples to be generated at the output layer. This corresponds to SNN 1 in Table I. The ACLR difference between spectra with SNN and AILC is mainly from the SNN error. A better training algorithm would help to reduce this gap. By reducing the number of the frequency samples with factor 2 and 4, we obtain SNN 2 and SNN 4. We can see that SNN 1 has the best linearization performance but it needs more power than SNN 2 and SNN 4. In scenarios with lower the linearity requirements, it is preferable to reduce the input frequency samples for lower power consumption.

To the authors' knowledge, this is the first time that emerging spiking neuron techniques are applied to the linearization of the PA network with LOS channel. The results show that this technique is promising, but further development is needed to refine this technique in terms of experimental implementation.

V. Conclusion

In this paper, we present a study on the power estimation of a two-layer SNN in linearizing a 10-PA array with LOS channel. The SNN is trained with data received through OTA observation. Different structures of SNN are evaluated on aspects of linearization accuracy and power consumption. Further study is to improve the training algorithm and to make experimental test with an antenna array in an anechoic chamber.

Acknowledgment

The authors would like to thank Jinhai Yuan for his work during internship.

REFERENCES

[1] A. Cappy, *Neuro-inspired Information Processing*, ser. Electronics Engineering Series. Wiley-ISTE, 2020.

[2] A. L. Hodgkin and A. F. Huxley, "A quantitative description of membrane current and its application to conduction and excitation in nerve," *J. Physiol.*, vol. 117, no. 4, pp. 500–544, Dec. 1952.

[3] L. H. Morris C, "Voltage oscillations in the barnacle giant muscle fiber," *Biophys J.*, vol. 35, no. 1, pp. 193–213, Jul. 1981.

[4] M. A. Nahmias, B. J. Shastri, A. N. Tait, and P. R. Prucnal, "A leaky integrate-and-fire laser neuron for ultrafast cognitive computing," *IEEE J. Sel. Top. Quantum Electron.*, vol. 19, no. 5, pp. 1–12, 2013.

[5] F. Danneville, C. Loyez, K. Carpentier, I. Sourikopoulos, E. Mercier, and A. Cappy, "A sub-35 pw axon-hillock artificial neuron circuit," *Solid-State Electronics*, vol. 153, pp. 88–92, 2019. [Online]. Available: https://www.sciencedirect.com/science/article/pii/S0038110118305562

[6] R. Borwankar, A. Desai, M. R. Haider, R. Ludwig, and Y. Massoud, "An analog implementation of fitzhugh-nagumo neuron model for spiking neural networks," in *2018 16th IEEE International New Circuits and Systems Conference (NEWCAS)*, 2018, pp. 134–138.

[7] P. M. Ferreira, N. De Carvalho, G. Klisnick, and A. Benlarbi-Delai, "Energy efficient fJ/spike LTS e-neuron using 55-nm node," in *2019 32nd Symposium on Integrated Circuits and Systems Design (SBCCI)*, 2019, pp. 1–6.

[8] C. Loyez, K. Carpentier, I. Sourikopoulos, and F. Danneville, "Subthreshold neuromorphic devices for spiking neural networks applied to embedded A.I," in *2021 19th IEEE International New Circuits and Systems Conference (NEWCAS)*, 2021, pp. 1–4.

[9] Y. Cao, Y. Chen, and D. Khosla, "Spiking deep convolutional neural networks for energy-efficient object recognition," in *International Journal of Computer Vision*, 2015, pp. 54–66.

[10] Z. Wang, Y. Zhang, S. Lian, X. Cui, R. Yan, and H. Tang, "Toward high-accuracy and low-latency spiking neural networks with two-stage optimization," *IEEE Transactions on Neural Networks and Learning Systems*, pp. 1–15, 2023.

[11] Y. Zhang, L. Wu, W. He, Z. Zhang, C. Yang, Y. Wang, Y. Wang, K. Tian, J. Liao, and Y. Yang, "An event-driven spatiotemporal domain adaptation method for dvs gesture recognition," *IEEE Transactions on Circuits and Systems II: Express Briefs*, vol. 69, no. 3, pp. 1332–1336, 2022.

[12] S. Wang, P. M. Ferreira, and A. Benlarbi-Delai, "Physics informed spiking neural networks: Application to digital predistortion for power amplifier linearization," *IEEE Access*, pp. 1–1, 2023.

[13] J. Wood, *Behavioral Modeling and Linearization of RF Power Amplifiers:*, ser. Artech House Microwave Library. Artech House, 2014.

[14] S. Wang, M. Roger, and C. Lelandais-Perrault, "Impacts of crest factor reduction and digital predistortion on linearity and power efficiency of power amplifiers," *IEEE Trans. Circuits Syst. II, Exp. Briefs*, vol. 66, no. 3, pp. 407–411, Mar. 2019.

[15] S. Wang, M. Roger, J. Sarrazin, and C. Lelandais-Perrault, "A joint crest factor reduction and digital predistortion for power amplifiers linearization based on clipping-and-bank-filtering," *IEEE Trans. Microw. Theory Techn.*, pp. 1–9, Dec. 2019.

[16] X. Wang, Y. Li, C. Yu, W. Hong, and A. Zhu, "Digital predistortion of 5g massive mimo wireless transmitters based on indirect identification of power amplifier behavior with ota tests," *IEEE Transactions on Microwave Theory and Techniques*, vol. 68, no. 1, pp. 316–328, 2020.

[17] A. Mammela and A. Anttonen, "Why will computing power need particular attention in future wireless devices?" *IEEE Circuits Syst. Mag.*, vol. 17, no. 1, pp. 12–26, Firstquarter 2017.

[18] J. Kim and K. Konstantinou, "Digital predistortion of wideband signals based on power amplifier model with memory," *Electronics Letters*, vol. 37, no. 23, pp. 1417–1418, Nov 2001.

[19] D. Morgan, Z. Ma, J. Kim, M. Zierdt, and J. Pastalan, "A generalized memory polynomial model for digital predistortion of RF power amplifiers," *IEEE Trans. Signal Process.*, vol. 54, no. 10, pp. 3852–3860, Oct. 2006.

[20] A. Zhu, J. Pedro, and T. Brazil, "Dynamic deviation reduction-based volterra behavioral modeling of RF power amplifiers," *IEEE Trans. Microw. Theory Techn.*, vol. 54, no. 12, pp. 4323–4332, Dec 2006.

[21] A. Zhu, "Decomposed vector rotation-based behavioral modeling for digital predistortion of RF power amplifiers," *IEEE Trans. Microw. Theory Techn.*, vol. 63, no. 2, pp. 737–744, Feb 2015.

[22] S. Wang, M. Abi Hussein, O. Venard, and G. Baudoin, "Optimal sizing of two-stage cascaded sparse memory polynomial model for high power amplifiers linearization," *IEEE Trans. Microw. Theory Techn.*, vol. 66, no. 9, pp. 3958–3965, Sep. 2018.

[23] S. Wang, M. Roger, J. Sarrazin, and C. Lelandais-Perrault, "Hyperparameter optimization of two-hidden-layer neural networks for power amplifiers behavioral modeling using genetic algorithms," *IEEE Microw. Wireless Compon. Lett.*, vol. 29, no. 12, pp. 802–805, Dec. 2019.

[24] A. S. Tehrani, H. Cao, S. Afsardoost, T. Eriksson, M. Isaksson, and C. Fager, "A comparative analysis of the complexity/accuracy tradeoff in power amplifier behavioral models," *IEEE Trans. Microw. Theory Techn.*, vol. 58, no. 6, pp. 1510–1520, June 2010.

[25] M. Besrour, S. Zitoun, J. Lavoie, T. Omrani, K. Koua, M. Benhouria, M. Boukadoum, and R. Fontaine, "Analog spiking neuron in 28 nm cmos," in *2022 20th IEEE Interregional NEWCAS Conference (NEWCAS)*, 2022, pp. 148–152.

[26] I. Sourikopoulos, S. Hedayat, C. Loyez, F. Danneville, V. Hoel, E. Mercier, and A. Cappy, "A 4-fj/spike artificial neuron in 65 nm cmos technology," *Frontiers in Neuroscience*, vol. 11, 2017. [Online]. Available: https://www.frontiersin.org/article/10.3389/fnins.2017.00123

[27] A. Saleh, "Frequency-independent and frequency-dependent nonlinear models of TWT amplifiers," *Communications, IEEE Transactions on*, vol. 29, no. 11, pp. 1715–1720, Nov 1981.

[28] A. Brihuega, L. Anttila, and M. Valkama, "Frequency-domain digital predistortion for OFDM," *IEEE Microw. Wireless Compon. Lett.*, vol. 31, no. 6, pp. 816–818, 2021.

[29] F. Ponulak and A. Kasinski, "Supervised learning in spiking neural networks with resume: Sequence learning, classification, and spike shifting," *Neural Computation*, vol. 22, no. 2, pp. 467–510, 2010.

[30] S. Wang, M. Roger, J. Sarrazin, and C. Lelandais-Perrault, "Augmented iterative learning control for neural-network-based joint crest factor reduction and digital predistortion of power amplifiers," *IEEE Trans. Microw. Theory Tech.*, vol. 68, no. 11, pp. 4835–4845, 2020.